



Application of photocatalysis for the decontamination of water contaminated with the Acid Orange 10 dye in the presence of TiO_2 under irradiation

Moussa Abbas^{a,*}, Mohamed Trari^b

^aLaboratory of Soft Technologies, Valorization, Physicochemistry of Biological Materials and Biodiversity (LTDVPMBB), Faculty of Sciences, University M'hamedBougara of Boumerdes, Boumerdes 35000, Algeria, Tel. +213 552408419; Fax: +213 21 24 80 08; email: m.abbas@univ-boumerdes.dz

^bLaboratory of Storage and Valorization of Renewable Energies, Faculty of Chemistry (USTHB), BP 32-16111 Algiers, Algeria, email: mtrari@usthb.dz

Received 10 September 2021; Accepted 3 January 2022

ABSTRACT

The photocatalytic degradation of the Acid Orange 10 was carried out in a static reactor used for direct photolysis under polychromatic external lighting. Acid Orange 10 (Orange G: OG), is used in silk, wool products and dyeing. It is a recalcitrant dye, which resist to oxidation and thermal degradation, and persists in the aquatic environment. The photodegradation is one of the most studied processes over the last two decades and its large-scale application has grown steadily. As we will see below, the entity that absorbs light is a semiconductor characterized by a narrow forbidden band. The photodegradation of OG onto TiO_2 material has been investigated at batch conditions. The effects of contact time (0–60 min), initial pH (3–11), adsorbent dose (0.1–1 g/L), and OG concentration (10–40 mg/L) on the OG oxidation by TiO_2 have been studied. High light intensity increases the degradation efficiency. The experimental results have shown that the photocatalytic efficiency is proportional to the dose of catalyst, which above a threshold value becomes almost constant and depends on the pH. The adsorption is an important step controlling the apparent kinetic constant of the photocatalysis. The photodegradation rate was favored for high OG concentrations in agreement with the Langmuir–Hinshelwood model with constants K_r and K_{ad} are respectively 0.4780 L mg/min and 0.7823 L/g. The degradation rates are pH and temperature dependent with a high degradation at high temperatures. TiO_2 has a better activity for the OG degradation, compared to many catalysts available in the literature.

Keywords: Photocatalytic; Acid Orange 10; Orange G; TiO_2 powder; Kinetics; Modeling

1. Introduction

The discharge of colored effluents is a common phenomenon in industries of textile, leather, plastics, paper, food and cosmetics. According to a first estimate, more than 10,000 different dyes and pigments are used industrially, and over 0.7 million tons of synthetic dyes are produced annually worldwide [1]. Among the available synthetic species, the azo dyes are the largest group used in the textile

industry with 60%–70% [2]. About 10%–25% of textile dyes are lost during dyeing process, and ~ 20% are directly discharged as water effluents in different environmental components [3]. Unfortunately, most dyes escape conventional wastewater treatment processes and persist in the environment due to their high stability to light, temperature, water, detergents, as well as chemicals and microbial attacks [4]. The discharge of dye-containing effluents into the aquatic environment is undesirable, not only because of their color, but also because their breakdown products are highly

* Corresponding author.

toxic [5–7], carcinogenic or mutagenic [8]. Therefore, many approaches were used for the dyes removal from effluents including adsorption [9–13], coagulation, ozone treatment, photo-Fenton, biological discoloration, hypochlorite treatment and advanced oxidation processes (AOPs) [14–19]. Generally, we can classify them into three categories: chemical, physical and biological methods, each having its advantages and disadvantages. For adsorption, the problem is only displaced and additional treatments are in fact necessary to separate the purified effluents or to regenerate the adsorbents. By contrast, the photochemical or photocatalytic processes of degradation have been found to be effective for such chemicals [20,21]. In recent years, AOPs have been studied for the treatment of textile effluents and the processes were based on powerful oxidizing agents such as hydroxyl and superoxide ($\cdot\text{OH}$ and $\text{O}_2^{\cdot-}$) radicals. The most common AOP mechanism involves the use of UV light in the presence of H_2O_2 , TiO_2 , O_3 and Fenton's reagent. This technique is one of the processes studied over the past 20 y and its large-scale application has grown steadily. The entity that absorbs the light is a semiconductor characterized by a narrow band gap semiconductor, in this respect, several photocatalysts have been tested: TiO_2 , ZnO , CeO_2 , BaTiO_3 , CdS , ZnS . TiO_2 is by far the most studied, because it exhibits photochemical stability and photocatalytic activity in a wide pH range. It has led to the degradation of different kinds of molecules and in particular dyes. It is used either in powder form or in a thin films deposited on different substrates. Dyes are known to cause allergic dermatitis, skin irritation, cancer and mutation. In this category, Acid Orange 10 (OG) is a typical acid azo dye used in the food and textile applications and has been detected in the discharged wastewater. It is a sulfonated azo molecule, used in silk, wool products as well as in the manufacture of in-wood ink and organic dye. There are relatively few

reports on the OG degradation and in the present article, it was attempted to determine its degradation by a combined process namely TiO_2/UV treatment. The degradation was studied to elucidate the effect of various operating parameters such as pH, initial dye concentration (C_0), TiO_2 dose and intensity/light source, in chamber surface in a batch photoreactor. The main objective of this study is to enhance the contribution of the heterogeneous photodegradation in the water decontamination such as: the effectiveness of the method, the economic cost of the study, the quality of the TiO_2 catalyst compared to others as well as its regeneration and finally to provide pilot tests on an industrial scale.

2. Materials and methods

The dye used in the present study is the Acid Orange 10 (OG), molecular weight $\text{C}_{16}\text{H}_{10}\text{N}_2\text{Na}_2\text{O}_7\text{S}_2$ and 452.38 g/mol purchased from Biochem–Chemopharma (purity 99.99%); the chemical and physical proprieties of OG are reported in Table 1. its UV/Visible spectrum (50 mg/L) at natural pH (≈ 5.8) has three bands of variable intensity at 248, 332 and 476 nm. The pH affects the behavior of OG in basic medium, where we observe a change in the color of the solution, turning from yellow ($\text{pH} < 11.5$) to orange red ($\text{pH} < 11.5$). Under these conditions, we noted relatively a significant decrease of the most intense band (476 nm). On the other hand, up to pH 11.5, we did not observe any change neither on the color (yellow) or the bands positions.

The stock solution was prepared by dissolving 1 g of OG in 1 L of double-distilled water and kept in the dark. The working solutions (10, 20 and 40 mg/L) were prepared daily by dilution of the stock solution. All other chemicals used were of analytical grade.

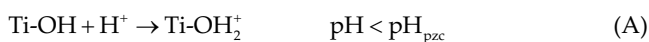
The heterogeneous photocatalysis is influenced by the pH, catalyst concentration, initial concentration (C_0) of

Table 1
General characteristics of Acid Orange 10 (OG)

Title	Properties
Dye name	Orange-G
Abbreviation	OG
Generic name	Acid Orange 10
Color Index (C.I.)	16,230 5
Appearance	Orange to red-orange powder
Chemical formula	$\text{C}_{16}\text{H}_{10}\text{N}_2\text{Na}_2\text{O}_7\text{S}_2$
Molecular Weight (g/mol)	452.37
λ_{max} (nm)	490
Toxic fumes	Carbon monoxide, carbon dioxide, nitrogen oxides, sulfur oxides
Chemical structure	

pollutant, light flux, ions in solution, crystallinity of the catalyst, etc. [22–25]. However, the interaction of these factors is not easy to control. The search for optimal conditions for removing pollutants is thus relatively complex because it depends on several factors.

TiO₂ purchased from Ahlstrom firm consists of Titania by Millennium inorganic chemicals. Fig. 1 gives the N₂ adsorption–desorption isotherm at 77 K on TiO₂; the insert shows the average pore size distribution calculated by the BJH equation of the desorption part of the isotherm. The average pore diameter distribution is ~ 5 nm, in the same range as the elementary particles. These pores correspond to interstices between the solid particles since the small single-crystal elementary particles are not porous on their surface. The characteristics of TiO₂ are the following: specific surface area 400 m²/g, p*H*_{pzc}: 6.5, crystalline phase containing 80% anatase and 20% rutile, and mean crystallites sizes in the range (5–10 nm). The p*H* determines the surface properties of solids as well as the state of the pollutant as a function of its p*K*_a and characterizes the water to be treated. In general, when a compound is partially ionized or carrying charged functions, it is necessary to consider the electrostatic interactions with TiO₂. p*H* is an important factor in photocatalysis and its variation modifies the surface charge of the catalyst, the speciation of the reagent and the balance of radicals reactions [26]. For all types of catalysts, there is always a p*H* called the zero charge point (pzc) where the surface charge is zero and can be determined experimentally. It depends on the catalyst and previous works showed the speciation of TiO₂ (pzc = 6.5) surface as a function of p*H* [27]. The reactions on the TiO₂ surface of are as follows:



The TiO₂ surface is positively charged in acidic solution related to the fixation of protons and negatively in basic medium (Fig. 2). The surface charge influences the dye adsorption and can either promote or inhibit the adsorption, depending on the p*H* value. Consequently, when the p*H* of the solution is different from p*H*_{pzc}, the surface is charged and this has a significant effect on the degradation rates. For neutral species, the degradation is almost insensitive to the p*H* variation. After 30 min. of shaking in the dark, to homogenize the suspension and allow rapid adsorption equilibrium, the irradiation was set up. Samples of 3 mL of suspension were taken as a function of time. The aliquots were filtered through cellulose acetate filters with a porosity of 0.45 mm. The filters are for single use under the following conditions: (Irradiation: 254 nm, lamp type used in the experiments: UV-C, *P* = 30 W and volume of the reactor is 1 L). The degradation was studied at three p*H*s, adjusted by addition of HCl (Merck, purity 97%) or NaOH (Carlo Erba, purity 98%). All solutions were prepared with bi-distilled water.

3. Results and discussion

3.1. Mechanism of photocatalysis

The absorption by the photocatalyst by energetic photons ($h\nu > E_g$) results in the formation of electron/hole (e^-/h^+) pairs respectively in the conduction band (CB) and valence band (VB) which constitute reactive radicals (resp. O₂^{•-} and [•]OH) responsible of the photodegradation of organic compounds. Hydroxyl radicals ([•]OH) are produced by oxidation of water or adsorbed hydroxide ions, depending on p*H*, on the semiconductor surface, while radicals are obtained from superoxide radical SO₂^{•-}, formed by reaction of O₂ with electrons [28]. The (e^-/h^+) pairs react with the molecules adsorbed on the TiO₂ surface. The photoelectrons can reduce an electron acceptor (oxidant) and the holes can oxidize an electron donor (reducer) (Fig. 3).

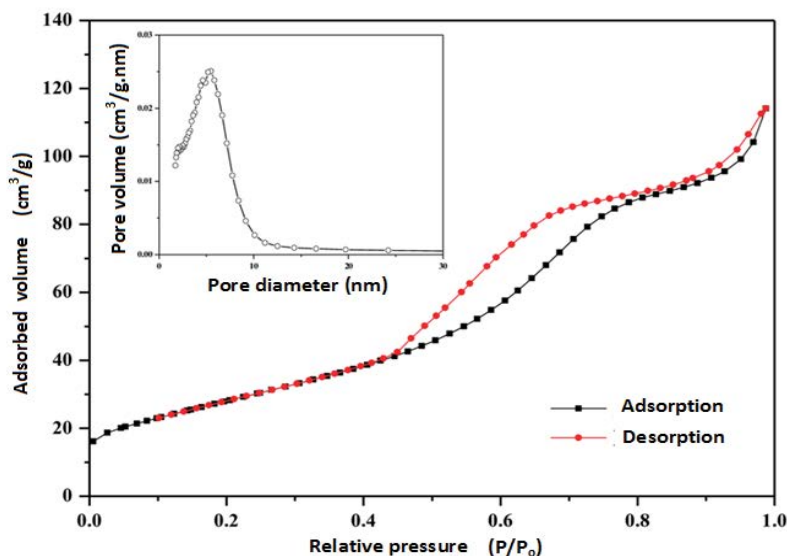
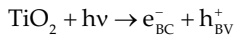
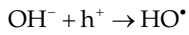


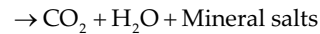
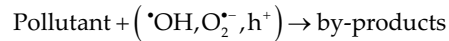
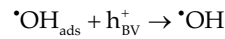
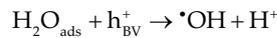
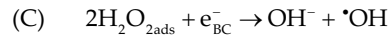
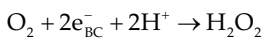
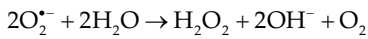
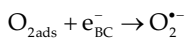
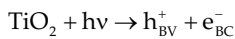
Fig. 1. The N₂ adsorption/desorption isotherms and pore size distribution curves of TiO₂.



The singlet oxygen and the superoxide ions play a secondary role in photocatalysis in the case of a highly hydrated or hydroxylated TiO_2 surface, trapping of h^+ gives surface-linked radicals HO^\bullet .



The photo degradation can occur by one or more active species and the overall mechanism on TiO_2 is as follows:



The degradation occurs mainly by $\bullet\text{OH}$, one of the most powerful oxidant ($2.3 \text{ V}_{\text{SHE}}$), generated by hole valence band process of TiO_2 (below), which react with the dye with a kinetic controlled by diffusion.

The heterogeneous photocatalysis is a complex process that is the subject of much research. As with any process including heterogeneous reactions, the photo-electrochemical process can be divided into five steps [29–31]:

- The transfer of reactive molecules dispersed in the fluid to the surface of the catalyst

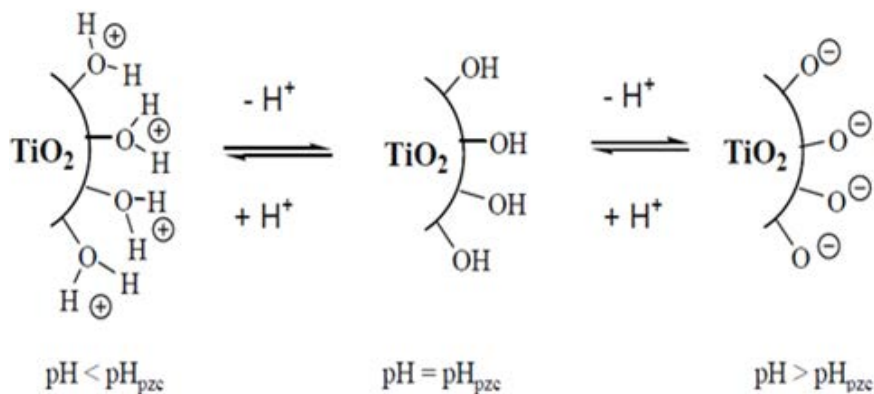


Fig. 2. Predominance charges in the photocatalyst TiO_2 .

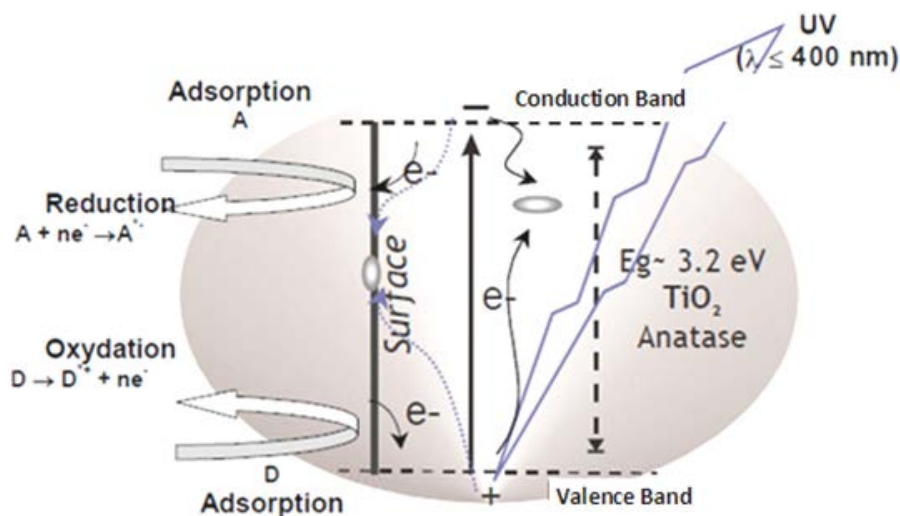


Fig. 3. Principle of photocatalysis.

- The adsorption of the reactive molecules on the TiO₂ surface of the catalyst
- Reaction on the surface of the adsorbed phase
- Desorption of the reaction products
- Removal of the reaction products from the interface solution/catalyst.

3.2. Photocatalysis of the Acid Orange 10

The photolysis of OG at 254 nm was carried out in aqueous medium with an initial concentration (C_0) equal to 50 mg/L in a static reactor. The pH initially measured is 5.8. The results obtained show that the compound is not photolysable at 254 nm. Thus, after 300 min of irradiation, the percentage of discoloration is only 5.3% but reached in the presence of TiO₂/UV an abatement of 95%. We also note that the OG solution has not undergone any change during these 300 min of direct photolysis (Fig. 4). The Mott–Schottky characteristic of TiO₂ indicates *n*-type compartment, due to oxygen vacancies, with a conduction band made up of Ti⁴⁺: 3d orbital ($-0.75 V_{SHE}$), more cathodic than the O₂/O₂⁻ level, yielding O₂⁻ formation. Concomitantly, the valence band derived from O²⁻: 2p character ($2.45 V_{SHE}$) is more anodic the [•]OH/H₂O level, thus yielding the formation of the radical [•]OH. The latter is mainly responsible of the OG oxidation [32]

4. Influence of analytical parameters

4.1. Effect of initial OG concentration

The experiments of OG discoloration by energetic photons (UV; 254 nm), that is, the photolysis was carried out at different concentrations C_0 in the range (10–40 mg/L). The optical density measurement was carried out at 476 nm, corresponding to the entity (–N=N–). The results obtained under these conditions allowed us to conclude that OG becomes photolysable when the dose in the substrate decreases (Fig. 5). In a restricted area of OG concentrations,

the reaction rate is proportional to the concentration C_0 , which follows a first order kinetic model. This is in agreement with the Langmuir–Hinshelwood (L-H) model if the solution is sufficiently diluted and/or the adsorption of the organic compound is weak. In this model, the determining step corresponds to the reaction of an adsorbed molecule with a reactive specie like [•]OH radical or photo hole (h^+) where a saturation is observed. Fig. 5 illustrates the results for different OG concentrations C_0 between 10 and 40 mg/L in the presence of TiO₂ (1 g/L) at free pH. The pace remains broadly unchanged from one concentration to another and we observe an exponential decay with a first order kinetic in all cases. As expected, the curves clearly show that the discoloration of the solution takes a longer time as long as the initial OG concentration is high. This observation results in a continuous decrease of the rate constant k (Table 2). Previous studies showed that the pollutant degradation by heterogeneous photocatalysis obeys rather the L-H model, where the degradation rate is proportional to the fraction of the catalyst surface covered by the substrate molecules and is given by [33]:

$$v = \frac{-dC}{dt} = \frac{K_r \cdot K \cdot C}{1 + K \cdot C} \quad (1)$$

For low concentrations ($C < 10^{-3}$ M), the term KC is negligible in front of 1. Therefore, the reaction follows a pseudo-first-order kinetic:

$$v = \frac{-dC}{dt} = K_r \cdot K \cdot C = K_{app} \cdot C \quad (2)$$

The integration of equation gives:

$$\ln \frac{C_0}{C} = K_{app} \cdot t \quad (3)$$

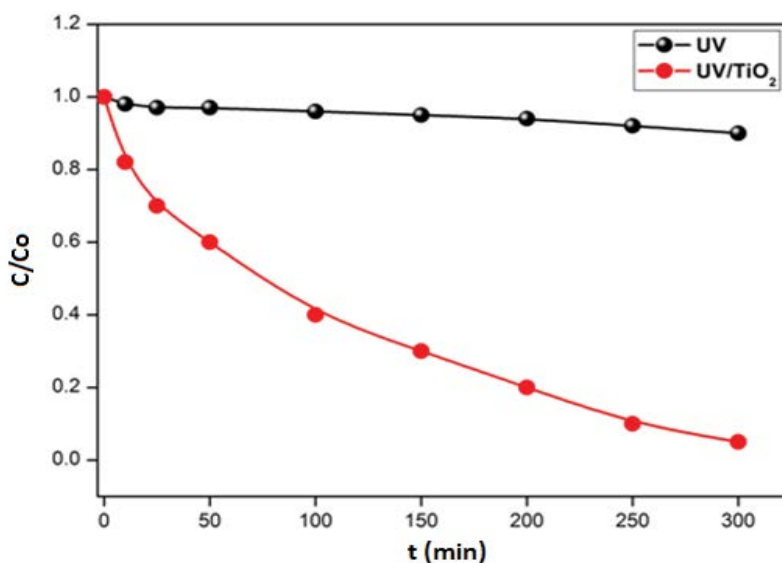


Fig. 4. Direct photolysis of the Acid Orange 10 (OG) (OG: 50 mg/L, $\lambda_{irr} = 254$ nm, $t = 300$ min).

The initial rate (v_o) is expressed by the relation:

$$v_o = \frac{K_r \cdot K \cdot C}{1 + K \cdot C} = K_{app} \cdot C_o \tag{4}$$

where v_o is the initial photodegradation rate (mg/L min), C the pollutant concentration at time t (mg/L), K_r the adsorption equilibrium constant (mg/L min), K the L-H kinetic constant (L/mg) and K_{app} ($=K_r \cdot K$) the apparent rate constant (min^{-1}) which is dependent on C_o . The plot $\ln(C_o/C)$ vs. t for different OG concentrations (C_o) and various catalyst amounts are illustrated in Fig. 6. The photocatalytic degradation follows perfectly the pseudo-first-order kinetic for in the C_o range (10–40 mg/L), the constants K_{app} (Table 2) indicate that the discoloration rate increases with raising C_o , in agreement with the L-H adsorption model. A linear expression is occasionally obtained by plotting K_{app}^{-1} against C_o :

$$\frac{1}{v_o} = \frac{1}{K_r} \cdot \frac{1}{C_o} + \frac{1}{K_r \cdot K} \tag{5}$$

4.2. Effect of mass of catalyst

The increase in the catalyst amount in suspension (Fig. 7) is synonymous with the augmentation of the illuminated surface, leading to a greater number of active sites and in this way to a large number of (e^-/h^+) pairs. Therefore and

as expected, a greater quantity of $\cdot\text{OH}$ with a better efficiency were obtained. However, beyond a threshold mass, which corresponds to the complete absorption of photons coming from the light source, a plateau region is reached which corresponds to a saturation of photo-electrochemical sites. This limit is function of the engineering and depends on the geometry of the reactor and the working conditions. It is therefore necessary to determine the optimum value for which the quantity of catalyst is minimal and the reaction rate is the greatest. Let's recall that, for higher catalyst doses, the reaction rate will even decrease due to the screen effect and possible agglomeration of the particles; the light scattering also accounts for the decline in the photoactivity. The plot $\ln(C_o/C)$ vs. t for different OG concentrations (C_o) and various catalyst amounts are illustrated in Fig. 8. The plot of $(1/v_o)$ against $(1/C_o)$ for OG and TiO_2 gives linear relationship (Fig. 9). From the slope ($1/K_r$) and the intercept ($1/K_r \cdot K$), the constants K_c and K for the photocatalytic degradation of OG and are deduced (Table 3).

4.3. Influence of light intensity

Our experimental device consists of an irradiation enclosure that can adapt one, two or three lamps as external light sources. This characteristic was used to examine the effect of the intensity of the incident photon flux (I_o) on the OG discoloration (5 mg/L). For this, we irradiated the OG dye by varying the power of the lamp. As expected, the

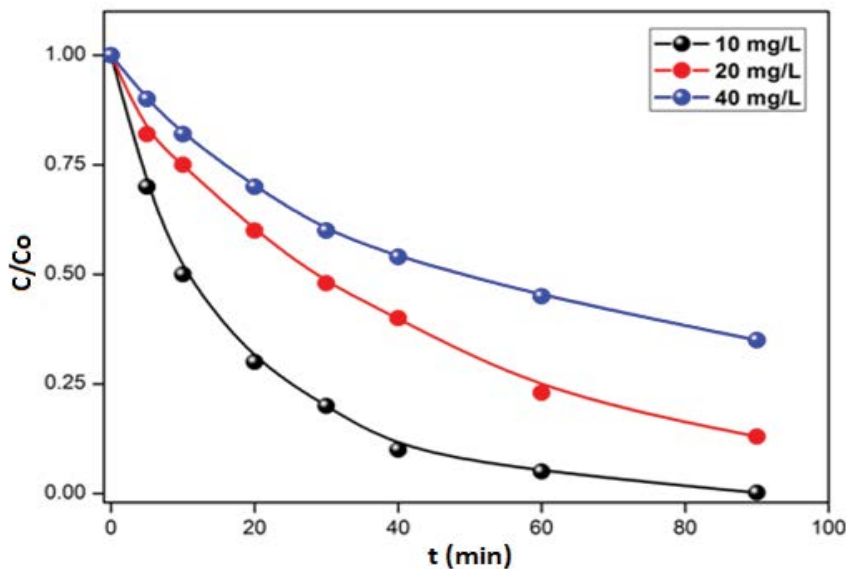


Fig. 5. Influence of the concentration of Acid Orange 10 on the kinetics of degradation (OG: 10–40 mg/L, $\lambda_{irr} = 254$ nm, $t = 300$ min, TiO_2 : 1 g/L).

Table 2
Determination of the degradation constants at different concentrations of Acid Orange 10 (OG)

$C_{o(\text{MO})}$ (mg/L)	K_{app} (min)	R^2	V_o (min g/L)	$C_{o(\text{TiO}_2)}$ (g/L)	K_{app} (min)	V_o (min g/L)	R^2
10	0.04237	0.9950	0.4237	0.1	0.0476	0.00476	0.9876
20	0.02248	0.9996	0.4496	0.5	0.00297	0.00297	0.9970
30	0.01154	0.9648	0.0.4617	1.0	0.000729	0.000729	0.9985

curves (Fig. 10) indicate that the percentage of elimination increases as the flux intensity increases. This result was predictable because of the higher number of incident photons and therefore a faster degradation of the dye OG.

4.4. Influence of pH

The influence of pH on the kinetic of OG degradation by heterogeneous photocatalysis has been studied at three pH (3, 7 and 10) adjusted by addition of HCl or NaOH (0.1M). The irradiation was carried out on solutions

with a OG concentration of 50 mg/L in presence of TiO_2 (1 g/L). The evolution of the initial degradation rates as a function of the pH (Fig. 11) indicates that the latter plays an important role in the kinetics of photodegradation. The pH effect is directly linked to the electrical state of the catalyst surface and the OG adsorption; its pzc is equal to 6.5. Indeed, in basic medium and knowing that the surface charge of TiO_2 is negative, OG with two sulfonic groups, is easily ionized and therefore becomes a soluble anion. There is therefore an attraction toward the OG which is thus far from the negative surface of TiO_2 . The

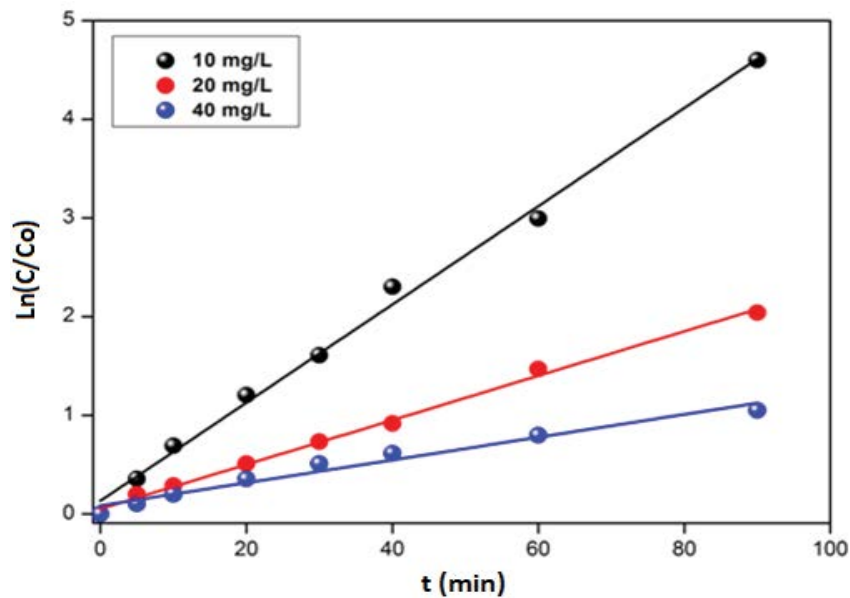


Fig. 6. Modeling of degradation kinetics according to the Langmuir–Hinshelwood model (L-H) (OG: 10–40 mg/L, $\lambda_{\text{irr}} = 254$ nm, $t = 300$ min, TiO_2 : 1 g/L).

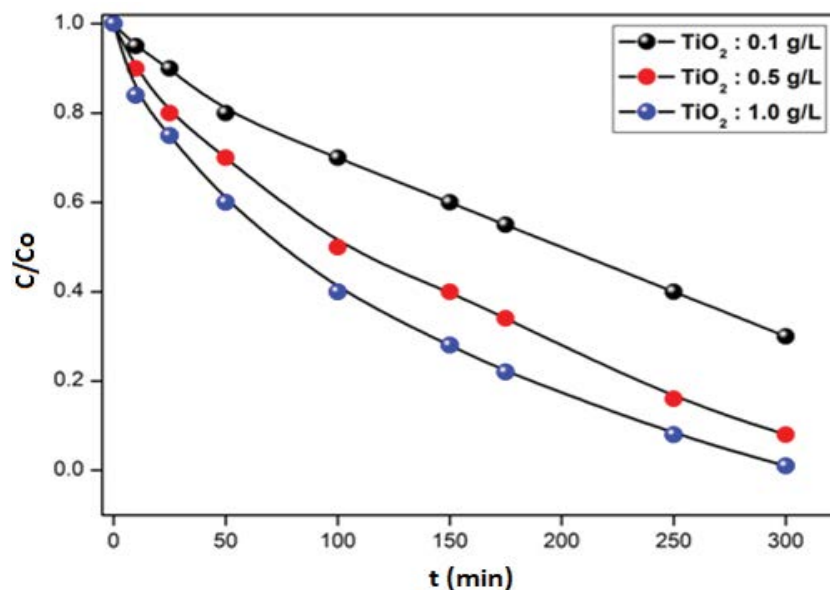


Fig. 7. Influence of the TiO_2 dose on the degradation kinetics. (OG: 50 mg/L; $\lambda_{\text{irr}} = 254$ nm, $t = 300$ min, TiO_2 : 0.1–1 g/L).

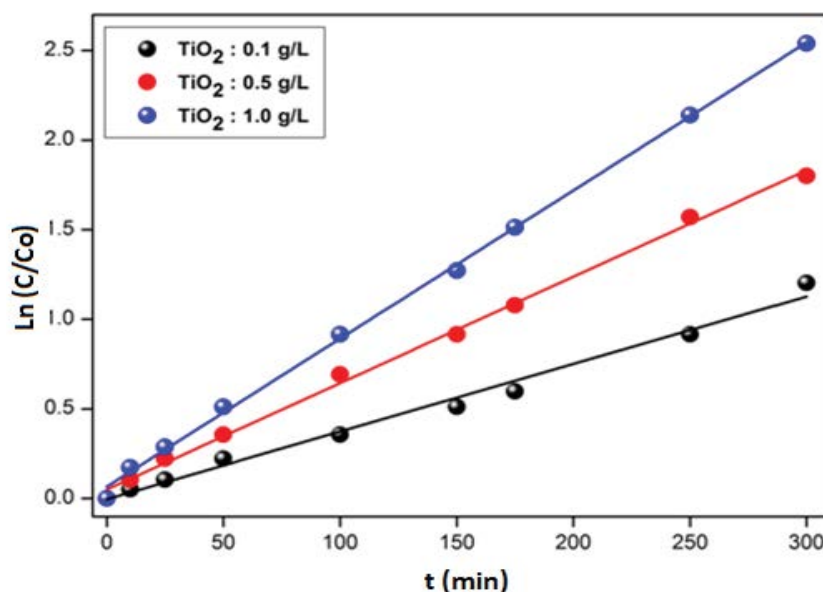


Fig. 8. Modeling of the degradation kinetics according to the Langmuir–Hinshelwood model (L-H) for the different doses of TiO_2 (TiO_2 : 0.1–1 g/L, $\lambda_{\text{irr}} = 254 \text{ nm}$, $t = 300 \text{ min}$, OG: 50 mg/L).

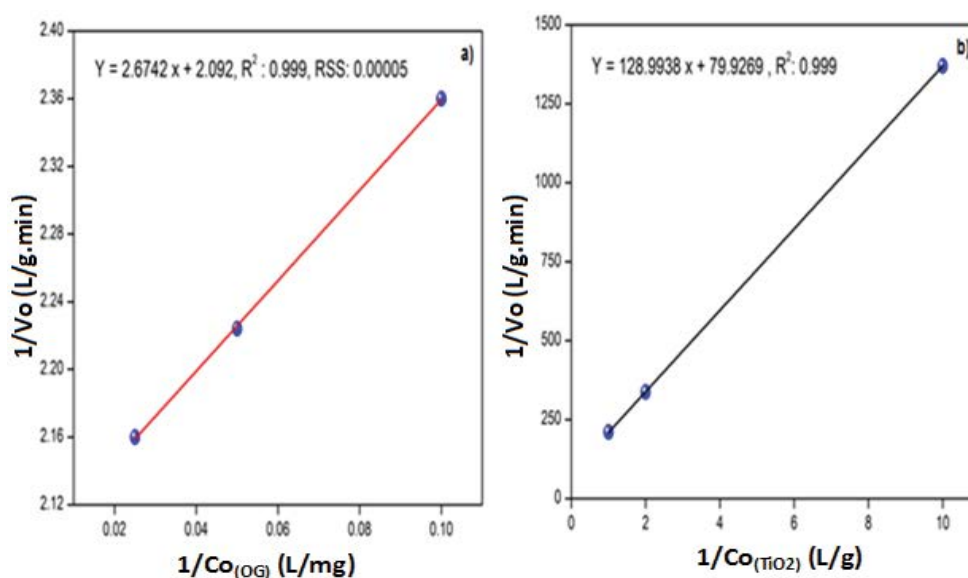


Fig. 9. Determination of photocatalytic constants. (a) (TiO_2 : 0.1–1 g/L, $\lambda_{\text{irr}} = 254 \text{ nm}$, $t = 300 \text{ min}$, OG: 50 mg/L) and (b) (OG: 10–40 g/L, $\lambda_{\text{irr}} = 254 \text{ nm}$, $t = 300 \text{ min}$, TiO_2 : 1 g/L).

existence of these attraction forces also leads to an increase in the photodegradation kinetic of this substrate at basic pH where we observe an enhance photoactivity.

5. Conclusion

The photocatalytic degradation of the Acid Orange 10 (OG) was carried out in a static reactor under polychromatic external lighting. This study has shown that TiO_2 can be employed as effective photocatalyst for the Acid Orange 10 removal, the adsorption equilibrium time was reached within 35 min. TiO_2 has a chemical stability over a wide

pH range and photoactivity towards various molecules, including dyes.

The elimination of solution of Acid Orange 10 (OG), an organic compound used in the textile industry, was carried out by adsorption/photo catalytic degradation. The advanced oxidation process involves the active species generated upon irradiation namely the radicals $\cdot\text{OH}$ and $\text{O}_2^{\cdot-}$. These specie induce highly oxidizing properties exploited for the destruction of the dye. Qualitative analysis performed immediately after the discharge revealed the presence in solution of mineral ions derived from the degradation of the parent molecule.

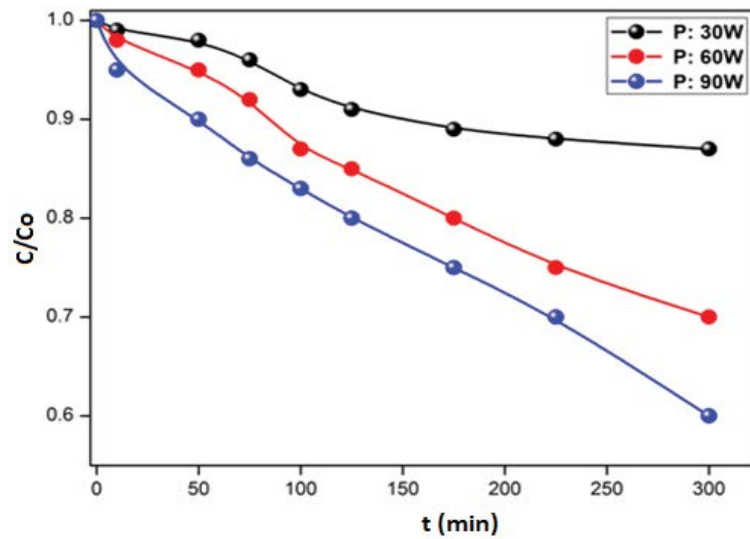


Fig. 10. Influence of the irradiation intensity on the degradation kinetics (OG: 5 mg/L; $\lambda_{\text{irr}} = 254 \text{ nm}$, $t = 300 \text{ min}$).

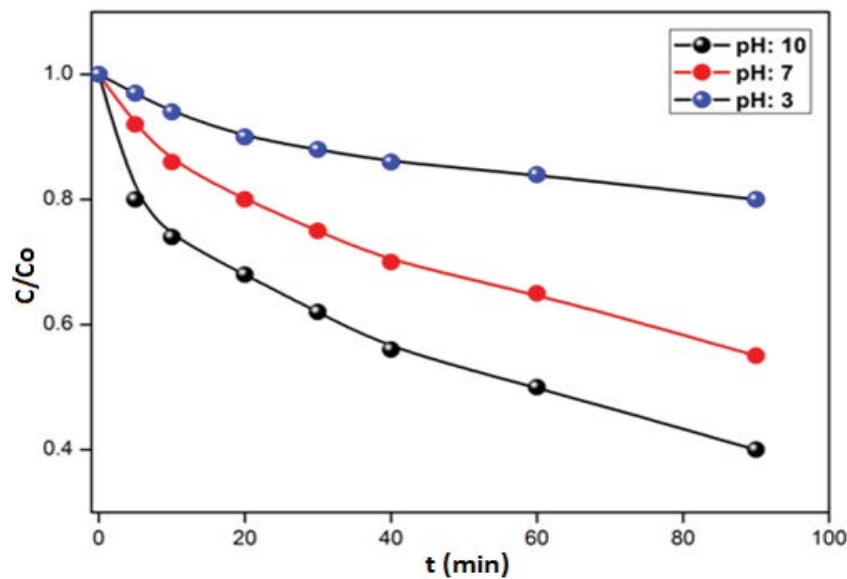


Fig. 11. Influence of pH on degradation kinetics (OG: 50 mg/L; $\lambda_{\text{irr}} = 254 \text{ nm}$, $t = 300 \text{ min}$, TiO_2 : 1 g/L).

Table 3
Adsorption and photocatalytic coefficients

Constants	Orange-G	TiO_2
K_r (L mg/min)	0.4780	0.0125
K_{ad} (L/g)	0.7823	0.6196

The photo degradation kinetic was affected by the initial OG concentration, in agreement with the Langmuir-Hinshelwood model. The parameters influencing the dye degradation are the pH, irradiation flux and catalyst dose. A better yield was obtained under optimal conditions (pH: 3, TiO_2 dose: 1 g/L, low concentration, and high light flux).

TiO_2 -based heterogeneous photocatalysis, used for water treatment, due to its advantages such as low cost, non-toxicity and efficiency under UV light. It promotes the photodegradation of a wide range of indoor pollutants at room temperature where the use of additives is not necessary.

Acknowledgements

The authors gratefully acknowledge support from University M'hamed Bougara of Boumerdes, Laboratory of Soft Technologies and Biodiversity, Faculty of Sciences. This research did not receive any specific grant from funding agencies in the public, commercial, or not-for-profit sectors.

Declaration of conflicting interests

The author(s) declared no potential conflicts of interest with respect to the research, authorship, and/or publication of this article.

References

- [1] T. Robinson, G. McMullan, R. Marchant, P. Nigam, Remediation of dyes in textile effluent: a critical review on current treatment technologies with a proposed alternative, *Bioresour. Technol.*, 77 (2001) 247–255.
- [2] R.G. Saratale, G.D. Saratale, J.S. Chang, S.P. Govindwar, Bacterial decolorization and degradation of azo dyes: a review, *J. Taiwan Inst. Chem. Eng.*, 42 (2011) 138–157.
- [3] M. Abbas, M. Trari, Contribution of adsorption and photocatalysis for the elimination of Black Eriochrome (NET) in an aqueous medium—optimization of the parameters and kinetics modeling, *Sci. Afr.*, 8 (2020) e00387, doi: 10.1016/j.sciaf.2020.e00387.
- [4] M. Abbas, T. Aksil, M. Trari, Removal of toxic methyl green (MG) in aqueous solutions by apricot stone activated carbon – equilibrium and isotherms modeling, *Desal. Water Treat.*, 125 (2018) 93–101.
- [5] M. Iqbal, *Vicia faba* bioassay for environmental toxicity monitoring: a review, *Chemosphere*, 144 (2016) 785–802.
- [6] M. Abbas, M. Adil, S. Ehtisham-ul-Haque, B. Munir, M. Yameen, A. Ghaffar, G. Abbas Shar, M. Asif Tahir, M. Iqbal, *Vibrio fischeri* bioluminescence inhibition assay for ecotoxicity assessment: a review, *Sci. Total Environ.*, 626 (2018) 1295–1309.
- [7] M. Iqbal, M. Abbas, J. Nisar, A. Nazir, A.Z. Qamar, Bioassays based on higher plants as excellent dosimeters for ecotoxicity monitoring: a review, *Chem. Int.*, 5 (2019) 1–80.
- [8] M. Abbas, Contribution of the electrocoagulation method in the removal of fluorine ions from aqueous solution, *Desal. Water Treat.*, 226 (2021) 177–183.
- [9] M. Abbas, Mass transfer processes in the adsorption of lead (Pb^{2+}) by apricot stone activated carbon (ASAC): isotherms modeling and thermodynamic study, *Prot. Met. Phys. Chem. Surf.*, 57 (2021) 687–698.
- [10] M. Abbas, A. Cherfi, S. Kaddour, T. Aksil, Adsorption in simple batch experiments of Coomassie blue G-250 by apricot stone activated carbon—kinetics and isotherms modelling, *Desal. Water Treat.*, 57 (2016) 15037–15048.
- [11] Z. Harrache, M. Abbas, T. Aksil, M. Trari, Thermodynamic and kinetics studies on adsorption of Indigo Carmine from aqueous solution by activated carbon, *Microchem. J.*, 144 (2019) 180–189.
- [12] M. Abbas, S. Kaddour, M. Trari, Kinetic and equilibrium studies of cobalt adsorption on apricot stone activated carbon, *J. Ind. Eng. Chem.*, 20 (2014) 745–751.
- [13] M. Abbas, Z. Harrache, M. Trari, Removal of gentian violet in aqueous solution by activated carbon equilibrium, kinetics, and thermodynamic study, *Adsorpt. Sci. Technol.*, 37 (2019) 566–589.
- [14] M. Abbas, M. Trari, Photocatalytic degradation of Asucryl Red (GRL) in aqueous medium on heat-treated TiO_2 powder – effect of analytical parameters and kinetic modeling, *Desal. Water Treat.*, 180 (2020) 398–404.
- [15] R.M.A. Aal, M.A. Gitru, Z.M. Essam, Novel synthesized near infrared cyanine dyes as sensitizer for dye sensitized solar cells based on nano- TiO_2 , *Chem. Int.*, 3 (2017) 358–367.
- [16] R. Arshad, T.H. Bokhari, T. Javed, I.A. Bhatti, S. Rasheed, M. Iqbal, A. Nazir, S. Naz, M.I. Khan, M.K.K. Khosa, M. Iqbal, M. Zia-ur-Rehman, Degradation product distribution of Reactive Red-147 dye treated by UV/ H_2O_2 / TiO_2 advanced oxidation process, *J. Mater. Res. Technol.*, 9 (2020) 3168–3178.
- [17] M. Abbas, Factors influencing the adsorption and photocatalysis of Direct Red 80 in the presence of a TiO_2 : equilibrium and kinetics modeling, *J. Chem. Res.*, (2021) 694–701, DoI: 10.1177/1747519821989969.
- [18] A. Jamil, T.H. Bokhari, T. Javed, R. Mustafa, M. Sajid, S. Noreen, M. Zuber, A. Nazir, M. Iqbal, M.I. Jilani, Photocatalytic degradation of disperse dye Violet-26 using TiO_2 and ZnO nanomaterials and process variable optimization, *J. Mater. Res. Technol.*, 9 (2020) 1119–1128.
- [19] M.A. Jamal, M. Muneer, M. Iqbal, Photo-degradation of monoazo dye blue 13 using advanced oxidation process, *Chem. Int.*, 1 (2015) 12–16.
- [20] M. Abbas, Experimental investigation of activated carbon prepared from apricot stones material (ASM) adsorbent for removal of malachite green (MG) from aqueous solution, *Adsorpt. Sci. Technol.*, 38 (2020) 24–45.
- [21] M. Abbas, M. Trari, Removal of methylene blue in aqueous solution by economic adsorbent derived from apricot stone activated carbon, *Fibers Polym.*, 21 (2020) 810–820.
- [22] R. Shen, K. He, A. Zhang, N. Li, Y.H. Ng, P. Zhang, J. Hu, X. Li, In-situ construction of metallic $Ni_3C@Ni$ core-shell cocatalysts over $g-C_3N_4$ nanosheets for shell-thickness-dependent photocatalytic H_2 production, *Appl. Catal., B*, 291 (2021) 120104, doi: 10.1016/j.apcatb.2021.120104.
- [23] Z. Liang, R. Shen, Y.H. Ng, P. Zhang, Q.J. Xiang, X. Li, A review on 2D MoS_2 cocatalysts in photocatalytic H_2 production, *J. Mater. Sci. Technol.*, 56 (2020) 89–121.
- [24] S. Wageh, A.A. Al-Ghamdi, R. Jafer, X. Li, P. Zhang, A new heterojunction in photocatalysis: S-scheme heterojunction, *Chin. J. Catal.*, 42 (2021) 667–669.
- [25] J. Wang, G. Wang, B. Cheng, J. Yu, J. Fan, Sulfur-doped $g-C_3N_4$ / TiO_2 S-scheme heterojunction photocatalyst for Congo Red photodegradation, *Chin. J. Catal.*, 42 (2021) 56–68.
- [26] Z. Harrache, M. Abbas, T. Aksil, M. Trari, Modeling of adsorption isotherms of (5,5'-disodium indigo sulfonate) from aqueous solution onto activated carbon: equilibrium, thermodynamic studies, and error analysis, *Desal. Water Treat.*, 147 (2019) 273–283.
- [27] C. Kormann, D.W. Bahnemann, M.R. Hoffmann, Photolysis of chloroform and other organic molecules in aqueous titanium dioxide suspensions, *Environ. Sci. Technol.*, 25 (1991) 494–500.
- [28] P.G. Kougiyas, I. Angelidaki, Biogas and its opportunities—a review, *Front. Environ. Sci. Eng.*, 12 (2018) 14, doi: 10.1007/s11783-018-1037-8.
- [29] A. Hamza, I.J. John, B. Mukhtar, Enhanced photocatalytic activity of calcined natural sphalerite under visible light irradiation, *J. Mater. Res. Technol.*, 6 (2017) 1–6.
- [30] A. Jamil, T.H. Bokhari, T. Javed, R. Mustafa, M. Sajid, S. Noreen, M. Zuber, A. Nazir, M. Iqbal, M.I. Jilani, Photocatalytic degradation of disperse dye Violet-26 using TiO_2 and ZnO nanomaterials and process variable optimization, *J. Mater. Res. Technol.*, 9 (2020) 1119–1128.
- [31] M.A. Jamal, M. Muneer, M. Iqbal, Photo-degradation of monoazo dye blue 13 using advanced oxidation process, *Chem. Int.*, 1 (2015) 12–16.
- [32] R. Brahimi, Y. Bessekhoud, A. Bouguelia, M. Trari, Improvement of eosin visible light degradation using PbS-sensitized TiO_2 , *J. Photochem. Photobiol. A*, 194 (2008) 173–180.
- [33] A. Hamza, I.J. John, B. Mukhtar, Enhanced photocatalytic activity of calcined natural sphalerite under visible light irradiation, *J. Mater. Res. Technol.*, 6 (2017) 1–6, doi: 10.1016/j.jmrt.2016.03.001.